International Journal of Nanomedicine

Dovepress
open access to scientific and medical research

Open Access Full Text Article

ORIGINAL RESEARCH

Synergistic Antitumor Efficacy Mediated by Liposomal Co-Delivery of Polymeric Micelles of Vinorelbine and Cisplatin in Non-Small Cell Lung Cancer

This article was published in the following Dove Press journal:
International Journal of Nanomedicine

Shuhang Wang[1]
Jingxin Gou[2]
Yue Wang[1]
Xinyi Tan[2]
Linxuan Zhao[1]
Xiangqun Jin[1]
Xing Tang[2]

[1]Department of Pharmaceutics, College of Pharmacy Sciences, Jilin University, Changchun, 130021, Jilin, People's Republic of China; [2]Department of Pharmaceutics Science, Shenyang Pharmaceutical University, Shenyang, 110016, People's Republic of China

Purpose: Non-small cell lung cancer (NSCLC) is an aggressive tumor with high mortality and poor prognosis. In this study, we designed a liposome encapsulating polymeric micelles (PMs) loaded with vinorelbine (NVB) and cis-diamminedichloroplatinum (II) (cisplatin or CDDP) for the treatment of NSCLC.

Materials and Methods: Sodium poly(α-L-glutamic acid)-graft-methoxy-polyethylene glycol (PLG-G-PEG_{5K}) was used to prepare NVB-loaded NVB-PMs and CDDP-loaded CDDP-PMs that were co-encapsulated into liposomes by a reverse evaporation method, yielding NVB and CDDP co-delivery liposomes (CoNP-lips) composed of egg phosphatidyl lipid-80/cholesterol/DPPG/DSPE-$mPEG_{2000}$ at a molar ratio of 52:32:14:2. The CoNP-lips were characterized in terms of particle size, zeta potential, drug content, encapsulation efficiency, and structural properties. Drug release by the CoNP-lips as well as their stability and cytotoxicity was evaluated in vitro, and their antitumor efficacy was assessed in a mouse xenograft model of Lewis lung carcinoma cell-derived tumors.

Results: CoNP-lips had a spherical shape with uniform size distribution; the average particle size was 162.97±9.06 nm, and the average zeta potential was −13.02±0.22 mV. In vitro cytotoxicity analysis and the combination index demonstrated that the CoNP-lips achieved a synergistic cytotoxic effect at an NVB:CDDP weight ratio of 2:1 in an NSCLC cell line. There was sustained release of both drugs from CoNP-lips. The pharmacokinetic analysis showed that CoNP-lips had a higher plasma half-life than NP solution, with 6.52- and 8.03-fold larger areas under the receiver operating characteristic curves of NVB and CDDP. CoNP-lips showed antitumor efficacy in tumor-bearing C57BL/6 mice and drug accumulation in tumors via the enhanced permeability and retention effect.

Conclusion: CoNP-lips are a promising formulation for targeted therapy in NSCLC.

Keywords: cisplatin, vinorelbine, co-delivery liposomes, combination therapy, polymeric micelles, non-small cell lung cancer

Introduction

Lung cancer is the most frequently diagnosed cancer; it is associated with a high rate of metastasis and poor prognosis, accounting for 18.4% of the total cancer deaths worldwide.[1] Approximately 85% of lung cancer cases are non-small cell lung cancer (NSCLC), which is extremely difficult to treat and has a very low survival rate.[2] Most NSCLC patients are diagnosed at an advanced stage of disease when the tumor(s) cannot be surgically resected or has spread to other tissues such

Correspondence: Xiangqun Jin
Department of Pharmaceutics, College of Pharmacy Sciences, Jilin University, Changchun, 130021, Jilin, People's Republic of China
Tel +86 431 85619252
Fax +86 431 85619662
Email jinxq@jlu.edu.cn

submit your manuscript | www.dovepress.com
DovePress
http://doi.org/10.2147/IJN.S290263

as lymph nodes and bone.[3,4] Immunotherapy has not significantly improved the prognosis of NSCLC because of low rates of efficacy; the 1-year survival rate for NSCLC is just 30%–35%, and approximately 80% of patients die within 5 years of diagnosis.[5]

Combination therapy is a common strategy for cancer treatment that allows dose reduction of individual drugs and the simultaneous treatment of multiple targets.[6,7] The combination of vinorelbine (NVB) and cis-diamminedichloroplatinum (II) (cisplatin or CDDP), referred to as NP, is a first-line treatment for many cancers.[8,9] Adjuvant NP is a standard chemotherapy for patients with early stage II or IIIA NSCLC[10,11] and was shown to improve median relapse-free and overall survival rates, with a 15% increase in 5-year survival compared to completely resected early-stage NSCLC.[12] However, NP is associated with hematologic and non-hematologic toxicities.[13] A highly targeted drug delivery system can improve the therapeutic effect of these drugs while reducing their side effects.

Advances in nanomedicine have yielded promising new strategies for the targeted treatment of solid tumors.[14] Poly(L-glutamic acid)-graft-methoxy-polyethylene glycol (PLG-g-mPEG) has been used with CDDP to generate polymer–metal complex nanoparticles (CDDP/PLG-g-mPEG) for cancer therapy.[15] Gemcitabine loaded onto PLG-g-mPEG via covalent bonding between its 4-amino group and the carboxyl group of PLG-g-mPEG showed good blood stability and prolonged circulation time.[16] PLG-g-mPEG was found to alter the water solubility of CDDP and cationic amphiphilic drugs, which reduced their side effects and improved therapeutic indices. Peptide-based delivery systems have also been investigated for platinum-based and cationic amphiphilic anticancer drugs.[17,18] Polymer entrapment enhances the solubility of drugs, prevents their interaction with the immune system, and can reduce their adverse effects.[2] Additionally, biodegradable polymers exhibit good clearance from the body, which increases their safety. The small size (<30 nm) of polymeric micelles (PMs) allows them to accumulate at the tumor site, and encapsulation into liposomes or polyethylene glycol (PEG)-liposomes protects drugs from chemical inactivation and enzymatic degradation,[19] thereby preserving their potency until delivery to target tissues via the enhanced permeability and retention (EPR) effect.[20,21]

Many types of liposome have been investigated as vehicles for the delivery of drug combinations.[22] For example, the recently approved liposome product CPX-351 encapsulating daunorubicin and cytarabine was evaluated for the treatment of acute myeloid leukemia; the co-delivered drugs were protected from metabolism and elimination and the differences in their pharmacokinetics were mitigated.[23] Doxorubicin and 5-fluorouracil encapsulated into a liposome by an ammonium-sulfate gradient method showed superior therapeutic effects in vivo compared to administration of the free drugs.[24] Tc-99m–radiolabeled and folate-targeted liposomes co-encapsulated with paclitaxel and NVB were associated with high rates of cellular uptake and cytotoxicity.[25] Compared to free drugs, liposome formulations encapsulating drug combinations had lower toxicity and inhibited tumor growth while reducing the rate of lung metastasis.[26] Thus, liposomes loaded with multiple drugs at an appropriate ratio allow synchronized drug delivery with controlled pharmacokinetics and biodistribution.

In the present study, we designed and synthesized liposomes for the co-delivery of NVB and CDDP (CoNP-lip) to achieve a synergistically enhanced antitumor effect in NSCLC (Figure 1). NVB and CDDP were first incorporated into their own PMs, which were then co-encapsulated into the same liposome formulation by a reverse evaporation method at a specific ratio that was calculated with the Chou–Talalay equation. As there have been previous reports investigating the interaction between PLG-g-mPEG with CDDP and amphiphilic cationic anticancer drugs and the use of CDDP-PMs, we have not described the preparation and characterization of CDDP- and NVB-PMs in detail here. Instead, we characterized the physicochemical properties of CoNP-lips including particle size, zeta potential, and loading efficiency; evaluated the controlled release of both drugs in vitro; and performed stability and cytotoxicity analyses. We also assessed the pharmacokinetics of CoNP-lips compared to a solution containing both drugs and the antitumor efficacy of CoNP-lips in vivo.

Materials and Methods

Materials, Cells, and Animals

CDDP was purchased from Kunming Guiyan Pharmaceutical Co. (Yunnan, China). NVB tartrate was from Guangzhou Baiyunshan Hanfang Pharmaceutical Co. (Guangzhou, China). 1,2-Distearoyl-sn-glycero-3-phosphoethanolamine-N-[methoxy(PEG)-2000] (DSPE-mPEG$_{2000}$), egg phosphatidyl lipid-80 (E80), and dipalmitoyl phosphatidylglycerol (DPPG) were from AVT Pharmaceutical Technology Co.

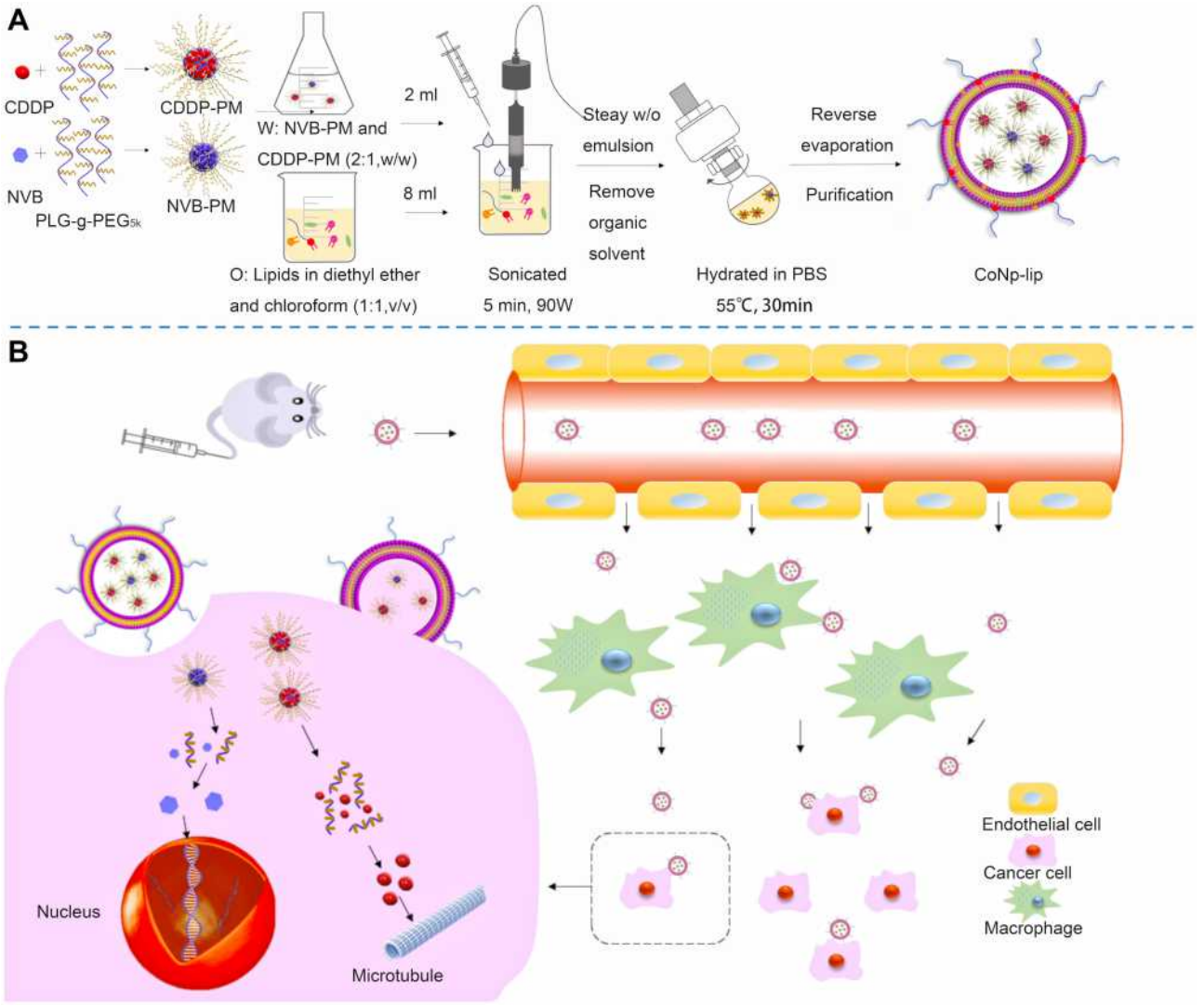

Figure 1 Co-encapsulation of NVB- and CDDP-PMs into liposomes. (**A**) A flowchart format of the preparation of CoNP-lips. (**B**) A schematic illustration of the structure, cellular uptake, and controlled drug release of CoNP-lips is shown.

(Shanghai, China). Cholesterol was from J&K Scientific (Beijing, China). Sodium poly (α-L-glutamic acid)-graft-methoxy-PEG (PLG-g-PEG_{5K}) (Mn: 30,000–40,000) was supplied by the Changchun Institute of Applied Chemistry (Changchun, China). 3-(4,5-Dimethylthiazol-2-yl)-2,5-diphenyltetrazolium bromide (MTT) was from Solarbio (Shanghai, China). Ketoconazole, the internal standard, was from Aladdin (Shanghai, China). High-glucose Dulbecco's modified Eagle's medium (DMEM), fetal bovine serum (FBS), and penicillin-streptomycin solution were from Hyclone (Logan, UT, USA). All other reagents were of analytical grade or higher and were obtained from commercial sources.

A549 human non-small cell lung cancer and Lewis lung carcinoma (LLC) cells were obtained from the Chinese Academy of Sciences Shanghai Cell Bank (Shanghai, China). The cell lines were cultured in high-glucose DMEM supplemented with 10% FBS, 1% penicillin, and 1% streptomycin at 37°C and 5% CO_2. Cultures were used for experiments when they reached 85–90% confluence.

Male Sprague–Dawley rats and C57BL/6 mice were obtained from the Experimental Animal Center of Shenyang Pharmaceutical University and maintained in a controlled environment with free access to water and food. Animal experiments were approved by the Animal Experimental Ethics Committee of Shenyang Pharmaceutical University and conformed to the guidelines of the committee. (Ethical number for Sprague–Dawley rats: SYPU-IACU-C2019-7-10-204, Ethical number for C57BL/6 mice: SYPU-IACUC-C2019-10-14-105.)

Determination of Combination Index (CI)

The cytotoxicity of CoNP-lips was evaluated with the MTT assay in A549 cells. The CI was calculated as the best synergy ratio between the 2 drugs according to the Chou–Talalay equation (Equation 1).

$$CI = (D)_1/(Dm)_1 + (D)_2/(Dm)_2 \quad (1)$$

In the equation, $(D)_1$ and $(D)_2$ represent the dose of each drug used in combination to achieve an effect, and $(Dm)_1$ and $(Dm)_2$ represent the dose of each drug used alone to achieve the same effect.[27]

A549 cells were seeded in 96-well plates (Costar 3599; Corning Inc, Corning, NY, USA) at a density of 5000/well and cultured overnight at 37°C in an incubator (Forma 3111; Thermo Fisher Scientific, Waltham, MA, USA). The cells were treated with CDDP (stock solutions with concentrations ranging from 0.01 to 100 $\mu g \cdot mL^{-1}$) and NVB (constant concentration) mixed at different weight ratios (1:1, 1:2, 1:3, 1:4, and 1:5). After 48 h, 20 μL of MTT (5 $mg \cdot mL^{-1}$) dissolved in phosphate-buffered saline (PBS) was added into each well, followed by incubation for 4 h at 37°C in the dark. After removing the supernatant, 100 μL of dimethylsulfoxide solution was added to dissolve the formazan crystals, and the absorbance of 570 nm was immediately measured with a microplate reader (SpectraMax 190; Molecular Devices, Sunnyvale, CA, USA).

Preparation and Characterization of CDDP-PMs and NVB-PMs

CDDP PMs were prepared with the self-assembly method.[28] CDDP and PLG-g-PEG_{5K} at a drug/copolymer ratio (w/w) of 1:3 were dissolved in deionized water with stirring (JJ-1; Wanfeng Manufacturing, Changzhou, China) for 24 h at 37°C in the dark. The mixture was concentrated using a tangential flow ultrafiltration membrane (ViavFlow 200; Sartorius, Göttingen, Germany) with a peristaltic pump (BT100-2J; Lange, Beijing, China), which was also used to remove unbound CDDP. NVB PMs were prepared via a 1-step self-assembly method.[29,30] NVB and PLG-g-PEG_{5K} at a drug/copolymer ratio (w/w) of 1:3 were dissolved in deionized water with stirring for 1 h at 37°C in the dark. The mixture was concentrated by centrifugation at 6000 rpm for 10 min using ultracentrifugal filters (Amicon Ultra-15; Millipore, Billerica, MA, USA) with a molecular weight cutoff (MWCO) of 10 kDa to remove unbound NVB. The particle size, size distribution, and zeta potential of the liposomes were determined by dynamic light scattering (DLS) (ZS-90 Zetasizer; Malvern Instruments, Malvern, UK). The encapsulation efficiency (EE) and drug loading (DL) of the 2 drugs were measured. Unencapsulated CDDP and NVB were removed by ultracentrifugation using a filter with an MWCO of 10 kDa, and the amount of CDDP and NVB was quantified by high-performance liquid chromatography (HPLC) (Chromaster 5000; Hitachi, Tokyo, Japan). CDDP analysis was conducted on a Luna NH_3 column (250 × 4.60 mm, i.d., 5μm, Phenomenex Corporation, Torrance, CA, USA). The HPLC mobile phase consisted of acetonitrile and water (75:20, v/v) at a flow rate of 0.8 $mL \cdot min^{-1}$, column temperature was maintained at 40°C, and injection volume was 20 μL. The detection wavelength was set at 310 nm.[28] Determination of NVB content was performed by HPLC at 249 nm, using a Zorbax C_{18} column (250 × 4.6 mm, i.d., 5 μm, Agilent Technologies, Santa Clara, CA, USA). The mobile phase was a mixture of acetonitrile and water (30 mM ammonium acetate adjusted to pH 3.2 using orthophosphoric acid, v/v = 55:45), and the flow rate was set at 1 $mL \cdot min^{-1}$, at ambient temperature.[31] Each measurement was carried out in triplicate. EE and DL were calculated according to the following equations.[32]

$$EE(\%) = W_{encapsulated\ drug}/W_{total\ drug} \times 100\% \quad (2)$$

$$DL(\%) = W_{encapsulated\ drug}/\left(W_{total\ drug} + W_{lipid}\right) \times 100\% \quad (3)$$

Preparation of NVB and CDDP Co-Delivery Liposomes (CoNP-Lips)

CoNP-lips were prepared using the previously described reverse evaporation method,[33] with some modifications. Briefly, 1 mL of CDDP-PMs (5 $mg \cdot mL^{-1}$ CDDP) and 1 mL of NVB-PMs (10 $mg \cdot mL^{-1} \cdot$NVB) were mixed as the water phase (2 mL). E80/cholesterol/DPPG/DSPE-$mPEG_{2000}$ at a molar ratio of 52:32:14:2 were dissolved in diethyl ether and chloroform (at a volume ratio of 1:1) as the oil phase (8 mL). The water phase was rapidly injected into the oil phase, followed by sonication for 5 min using a probe-ultrasonic cell disruptor (90 W) (JY-92-II; Xinzhi, Taizhou, China) without emulsion. The organic solvent was removed under reduced pressure at 45°C, yielding a viscous gel that was hydrated in PBS (0.01 M, pH 7.4) with stirring at 55°C for 30 min. The lipid suspension was passed through a 200-nm polycarbonate membrane 20 times using a hand-held LiposoFast basic

extruder (Avestin, Ottawa, ON, Canada). Unentrapped micelles were removed by ultra-high-speed refrigerated centrifuge (HC-3018R, Zhongke Zhongjia Scientific Instrument Co., Hefei, China) at 16000rpm, for 1 h. The liposome concentrates were stored at 4°C.

Preparation of liposome-encapsulated CDDP-PMs (CDDP-lip) and NVB-PMs (NVB-lip) was same with CoNP-lips (Supplementary Data). The optimal preparation conditions of CoNP-lips were determined using Design Expert v8.0.6 software (Stat-Ease, Minneapolis, MN, USA) (Supplementary Table 1).

Liposome Characterization

Particle size, size distribution, and zeta potential of CoNP-lips were evaluated by DLS. CoNP-lips were diluted with a 0.9% saline solution and triplicate measurements were carried out at 25°C. The morphology of the liposomes was visualized by transmission electronic microscopy (TEM) (JEM-2100; JEOL, Tokyo, Japan). Samples were mounted onto copper grids and stained with phosphotungstic acid (2%, w/v) for 2 min, then allowed to dry naturally for viewing.[34] An accelerating voltage of 200 kV was used. The EE and DL of both drugs were measured and CDDP and NVB contents were determined by HPLC. Each measurement was performed in triplicate.

Stability of CoNP-Lips in Different Media

CoNP-lips were diluted 20-fold in PBS (0.01 M, pH 7.4) and 10% plasma at 37°C with shaking at 100 rpm. At predetermined time points (0, 2, 4, 8, 12, 24, 48, and 72 h), particle size, polydispersity index (PDI), and EE were measured for the preliminary selection to determine the stability of CoNP-lips.

In vitro Release

The in vitro release of CDDP and NVB from CoNP-lips was determined with the dialysis method. Free CDDP, free NVB, CDDP-PM, NVB-PM, and CoNP-lips were incubated in PBS (pH 7.4 with 0.1 M NaCl) and 10% plasma at 37°C with stirring at 100 rpm. A 1-mL volume of each solution was transferred to a dialysis bag (Biosharp, Hefei, China) separately with an MWCO of 3.5 kDa that was incubated in 20 mL of release medium. At predetermined time points (0.5, 1, 2, 4, 8, 12, 24, and 48 h), 1 mL of sample was removed from the dialysis bag and replaced with pre-warmed fresh medium. The released drugs were quantified by HPLC and the release data were fitted to four mathematical models, including zero-order ($M_t/M_\infty = kt$), first-order ($\ln(1 - M_t/M_\infty) = -kt$), Higuchi ($M_t/M_\infty = kt^{1/2}$) and Ritger–Peppas ($M_t/M_\infty = kt^n$) models by using MATLAB (R2020a, MathWorks, Inc., Natick, MA, USA), where M_t represented drug accumulative release at time t, M_∞ represented drug accumulative release at time ∞, k represented the release rate constant, and n represented the diffusional exponent characteristic of the release mechanism. Results are presented as the mean ±SD of 3 test runs, and all measurements were performed in triplicate.

Cell Cytotoxicity Assay

A549 and LLC cells were seeded in 96-well plates (5000 and 10,000 cells/well, respectively) and cultured overnight, then exposed to blank liposomes, a CDDP and NVB mixed solution (NP-sol), a CDDP-PMs and NVB-PMs mixed solution (NP-PMs) and CoNP-lips (0.01, 0.1, 1, 5, 10, 50, and 100 $\mu g \cdot mL^{-1}$) at 37°C and 5% CO_2 for 48 h. The concentrations of NP-sol, NP-PMs and CoNP-lips were based on CDDP. Cell viability was evaluated with the MTT assay. The experiment was performed in triplicate. CalcuSyn v2.0 software (Biosoft, Cambridge, UK) was used to calculate the half-maximal inhibitory concentration (IC_{50}).

Pharmacokinetic Study

Male Sprague–Dawley rats (180–220 g) were randomly assigned to 2 groups (5 rats each). Rats were administered NP-sol or CoNP-lips via tail vein injection. Approximately 0.8 mL of blood from each rat was collected in heparinized tubes at predetermined time points (0.083, 0.5, 1, 2, 4, 8, 12, 24, and 48 h). Plasma was obtained by centrifugation at 6000 rpm for 10 min and divided into 2 parts that were stored at −20°C until analysis. CDDP content was measured by atomic absorption spectrophotometry (Analytic Jena AG, Jena, Germany). 100 µL plasma was mixed with 2 mL of a mixture of nitric acid and perchloric acid (v/v = 9:1). After soaking overnight, the intelligent sample processor (VB77, Leibtec Instrument Co., Beijing, China) was used for digestion at 140°C for 6 h. Then, 0.2 mL of distilled water was added and diluting with 0.2% nitric acid to 1 mL for measurement.[28] NVB content was measured by ultrahigh-performance liquid chromatography–mass spectrometry. The separation was carried out on an ACQUITY UPLCTM BEH C18 column (50 × 2.1 mm i.d., 1.7 µm; Waters, Milford, MA, USA) with the column temperature maintained at 35°C. The mobile phase consisted of (A)

acetonitrile and (B) water (containing 0.02 M ammonium acetate) and was delivered at a flow rate of 0.2 mL/min. The column was kept at 35°C, and the autosampler was maintained at 4°C. The linear gradient elution program was (1) A decreased from 60% to 20% during the first 0.5 min; (2) A was held at 30% for 0.7 min; (3) A was reset to the initial composition in 0.6 min; (4) A was held at 80% for 0.8 min. The injection volume was 5 μL using the partial loop mode. A Waters ACQUITY™ TQD triple-quadrupole tandem mass spectrometer (Waters, Manchester, UK) with an ESI interface was connected to the UPLC system. The optimized source/gas parameter was capillary 1.5 kV; cone voltage 3.0 V; radio frequency 0.1 V; source temperature 100°C; desolvation temperature 400°C. Nitrogen was used as the desolvation gas (500 L/h) and cone gas (50 L/h). For collision-induced dissociation, argon was used as the collision gas at a flow rate of 0.15 mL/min. The fragmentation transitions for MRM were m/z 779.38→122.11 amu for NVB, and m/z 531.11→82.07 amu for IS (ketoconazole), with a scan time of 0.02 s per transition. Pharmacokinetic data were collected by Masslynx™ NT4.1 software (Waters Corp., Milford, MA, USA) and processed with the QuanLynx™ program (Waters Corp, Milford, MA, USA).[35] Pharmacokinetic parameters were calculated using DAS v2.0 software (Mathematical Pharmacology Professional Committee of China, Shanghai, China).

In vivo Antitumor Efficacy

Male C57BL/6 mice bearing LLC cell-derived tumors were used to investigate the in vivo antitumor efficacy of the CoNP-lips. Mice were inoculated in the right flank with 1×10^7 LLC cells. When the tumor volume reached 180–200 mm^3, the mice were divided into 5 groups. Normal saline (NS), liposome-encapsulated CDDP (CDDP-lip; 5 $mg\cdot kg^{-1}$) and NVB (NVB-lip; 10 $mg\cdot kg^{-1}$), NP-sol (5 $mg\cdot kg^{-1}$ CDDP and 10 $mg\cdot kg^{-1}$ NVB), and CoNP-lips (5 $mg\cdot kg^{-1}$ CDDP and 10 $mg\cdot kg^{-1}$ NVB) were intravenously injected into the tail vein every 2 days for a total of 3 times. Starting after the first administration, body weight and tumor volume were recorded every 2 days to assess treatment efficacy and toxicity. Mice in each group (n=3) were sacrificed at 10 min, 1 h, and 48 h after administration to assess the accumulation of CDDP and NVB in the tumor. At 14 days after the first injection, mice were sacrificed and the tumors were excised, weighed, and photographed (n=5). Tumor size was measured using digital calipers (MNT-150T; Jingping, Shanghai, China) and the volume is calculated using Equation 4:

$$V = \frac{1}{2} \times \left(a \times b^2\right) \tag{4}$$

where a and b are the length and width of the tumor, respectively. Tumor inhibition rate (TIR) is calculated using Equation 5:

$$TIR(\%) = \left(1 - W_{drug}/W_{control}\right) \times 100\% \tag{5}$$

where W_{drug} and $W_{control}$ are the average tumor weights of the drug-tested group and the NS (control) group, respectively.

Statistical Analysis

Data are presented as mean±SD. SPSS v17.0 (SPSS Inc, Chicago, IL, USA) was used for statistical analyses. Differences between groups were evaluated with the Student's *t*-test; p values <0.05 were considered statistically significant.

Results and Discussion

CI Evaluation

NVB functions by disrupting the microtubule network and inducing G2/M phase arrest and caspase-3 activation,[36] while the anticancer activity of CDDP involves binding to DNA to create lesions that lead to cell cycle (G1, S, and G2 phases) and DNA replication arrest and necrosis or apoptosis.[37] Thus, the NP combination acts on cancer cells via distinct mechanisms and at different times, thereby exerting an enhanced antitumor effect compared to either drug alone.[38]

We evaluated the toxicity of the drugs in A549 cells treated with NVB and CDDP at different weight ratios for 48 h. Higher drug concentrations decreased cell viability in a dose-dependent manner in the MTT assay (Figure 2A). Compared to single-drug treatment, combination therapy had a more potent antitumor effect at high doses. A549 cells were more sensitive to NVB than CDDP, with IC_{50} values of 7.451±2.044 and 10.649±3.161 $\mu g\cdot mL^{-1}$, respectively. CI provides a quantitative measure of how 2 drugs interact, with values <1, equal to 1, and >1 indicating synergism, additive effects, and antagonism, respectively.[27] The CI values of all groups were <1 (Figure 2B). Maximum synergism was observed at a ratio of 2:1, with a CI value of 0.257. Based on CI and IC_{50} values and the results of the cell viability assay, an NVB:CDDP ratio of 2:1 was selected for subsequent experiments.

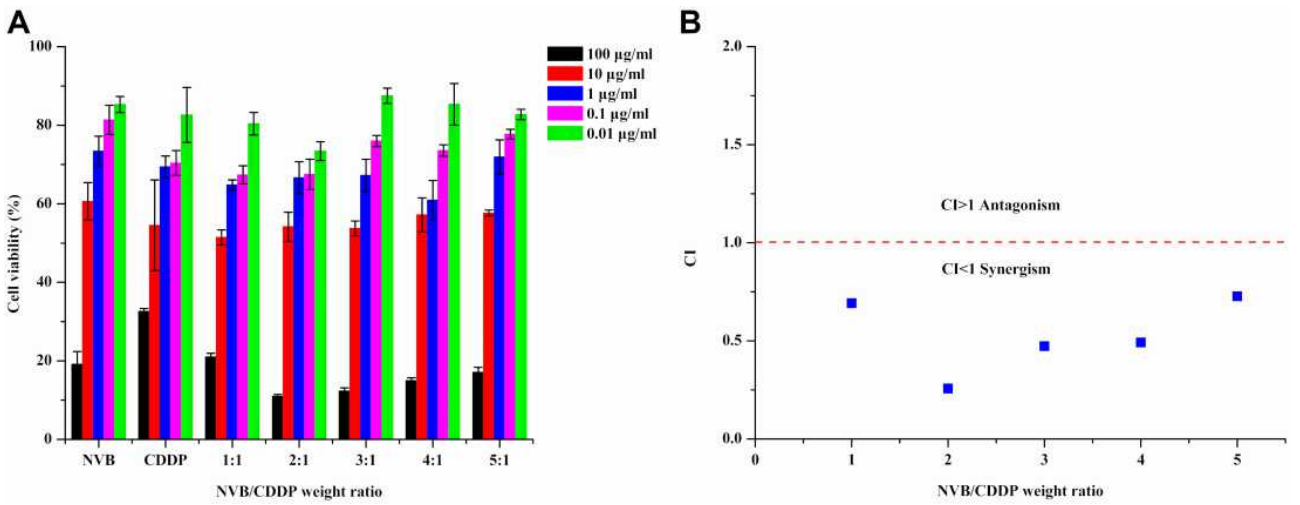

Figure 2 Cytotoxicity of NVB and CDDP. (**A**) Viability of A549 cells exposed to different weight ratios of NVB and CDDP for 48 h. (**B**) CI values at different weight ratios of NVB and CDDP as a measure of synergistic cytotoxicity. The concentration of the mixture was based on that of CDDP. Data are shown as mean±SD (n=3).

Preparation and Characterization of CDDP-PMs and NVB-PMs

CDDP-PMs were prepared based on the formation of a polymer–metal complex between CDDP and PEG–polyglutamic acid (PGA) graft copolymers (Figure 3A). PLG-g-PEG_{5K} provided COO^-, which replaced Cl^- and formed a coordination bond with platinum. CDDP in water formed hydrated platinum upon heating, which facilitated the reaction with PLG-g-PEG_{5K}. The COO^- of PGA formed a complex with CDDP, with the PEG chain exposed on the outside. As NVB is a cationic amphiphilic drug, it is possible that it can be encapsulated by PLG-g-PEG_{5K} through electrostatic interactions where the micelles have a negative charge in addition to being amphiphilic.[29] NVB is known to cause venous irritation and phlebitis when intravenously administered; encapsulation into PMs can reduce these side effects.[39]

We speculated that because of the addition of a copolymer, NVB- PMs and CDDP-PMs would have similar structures and physicochemical properties as well as comparable DL and release behaviors when encapsulated into liposomes. Structural analysis of PLG-g-PEG_{5K} revealed that CDDP formed a complex while NVB engaged in electrostatic interactions with the copolymer. The TEM analysis and particle size distribution showed that CDDP- and NVB-PMs had a near-spherical morphology (Figures 3 and 4), with particle sizes of 14.57±0.45 and 24.95±1.14 nm, respectively (Table 1).

Preparation and Characterization of CoNP-Lips

CoNP-lips were prepared via a reverse evaporation method. The liposomes had a uniform particle size <200 nm with a PDI <0.2 (Table 2, Supplementary Table 2), making them suitable for intravenous injection. The particle size of CoNP-lips was 162.97±9.06 nm; thus, the loading of CDDP- and NVB-PMs resulted in a slight increase in size (Figure 5). The zeta potential of blank liposomes and CoNP-lips was −15.07±0.19 and −13.02 ±0.22 mV, respectively. The negative zeta potentials were attributable to the negatively charged lipids, which may have increased the stability of the liposomes over the short term.

As the CoNP-lips were prepared through reverse evaporation, the EE of CDDP was the same as that of NVB (59.63% ±1.53% and 52.61%±2.21%, respectively) (Table 2). At an NVB:CDDP weight ratio of 2:1, the similar EE resulted in similar DL, 2.14%±0.054% for CDDP and 3.72%±0.15% for NVB, which was close to the ideal ratio.

The Box-Behnken design (BBD) (Supplementary Tables 3 and 4) and response surface methodology (RSM) (Supplementary Figure 1) were employed to analyze the compositions of cholesterol, DPPG and DSPE-$mPEG_{2000}$ (Supplementary Tables 3 and 4, Supplementary Figure 1). The optimal molar ratio of composition was therefore confirmed to be E80: cholesterol: DPPG: DSPE-mPEG2000, 52: 32: 14: 2.

DPPG is an anionic lipid that is an important component of Lipoplatin, a liposome–CDDP formulation that is

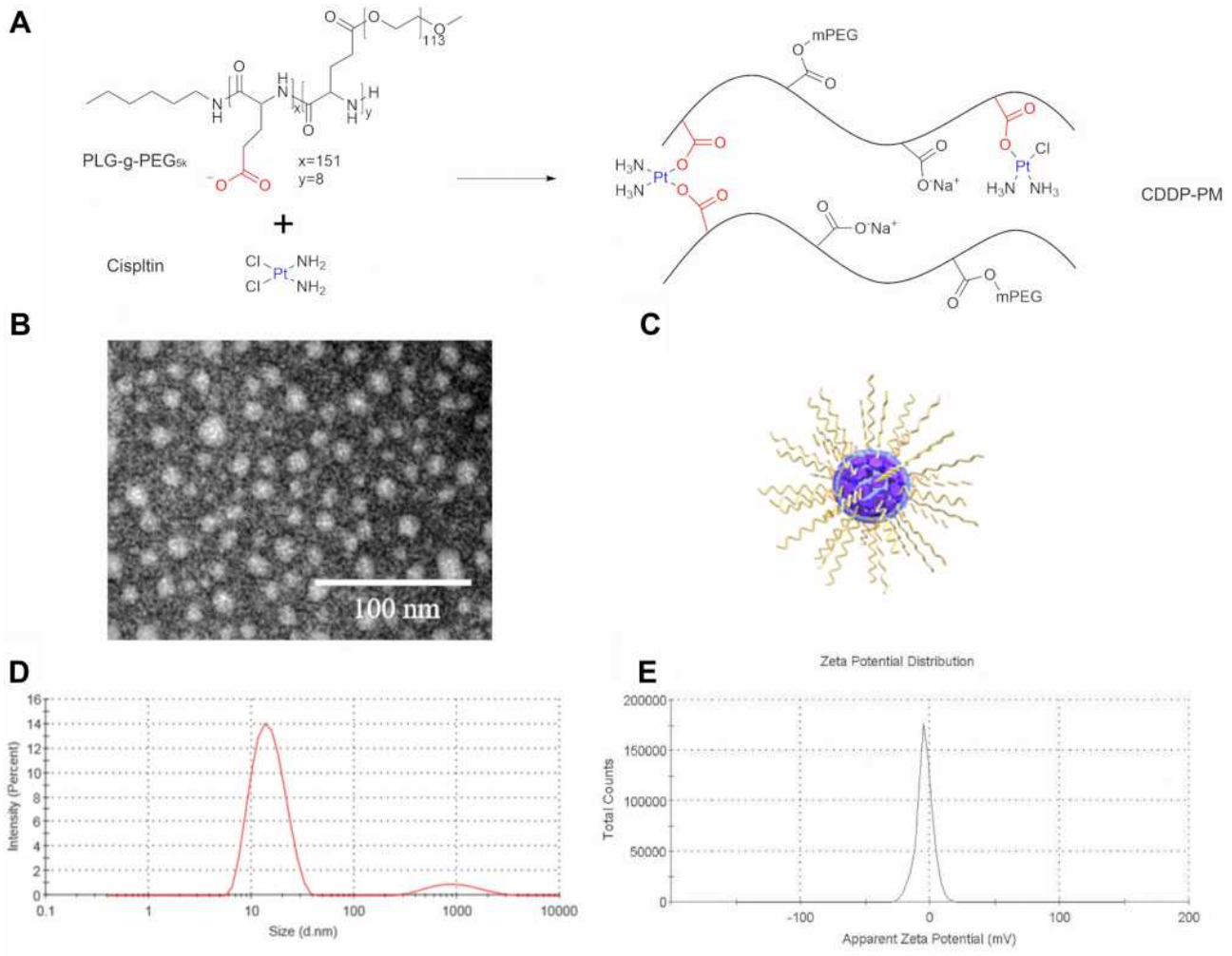

Figure 3 Chemical structures of synthesized and characterization of CDDP-PMs. (**A**) Chemical structures of synthesized, (**B**) TEM image, (**C**) schematic illustration, (**D**) size distribution, and (**E**) zeta potential of CDDP-PMs. Scale bar, 100 nm.

currently being evaluated in clinical trials. DPPG stabilizes liposomes and improves therapeutic efficacy through its fusogenic properties,[39,40] which promote cell fusion of the liposomes rather than their endocytosis. Additionally, a higher concentration of DPPG enhances interactions with the lipid bilayer although an excess can lead to liposome destabilization.[39,41]

Stability of CoNP-Lips in Different Media

We evaluated the stability of CoNP-lip in PBS (pH 7.4) and 10% plasma. In PBS, the average particle size did not change significantly but PDI increased slightly with prolonged incubation, indicating that the particles could accumulate when stored for over 72 h (Figure 6A). CoNP-lips were stable in PBS solution for up to 72 h, and the EE of CDDP in the CoNP-lips did not change over this time period in PBS (Figure 6B). However, the EE of NVB in the CoNP-lips declined over time both in PBS and 10% plasma. Given the weakness of electrostatic interactions between NVB and PLG-g-PEG$_{5K}$, NVB-PMs are more likely to break down when the liposomes accumulate. In 10% plasma, particle size and PDI increased slightly with prolonged incubation as well (Figure 6C). EE of CDDP and NVB in the CoNP-lips declined after 12 h (Figure 6D). In this work, PBS (pH 7.4) and 10% plasma were selected as the medium for in vitro release study.

In vitro Drug Release

Over 85% CDDP was rapidly released from the drug solutions before reaching a plateau at 6 and 8 h, respectively (Figure 7A). When they were encapsulated, the amounts of CDDP-PMs and NVB-PMs released at 48 h were much lower than those of the free drugs. Approximately 17.87±1.54% of the CDDP and 56.96

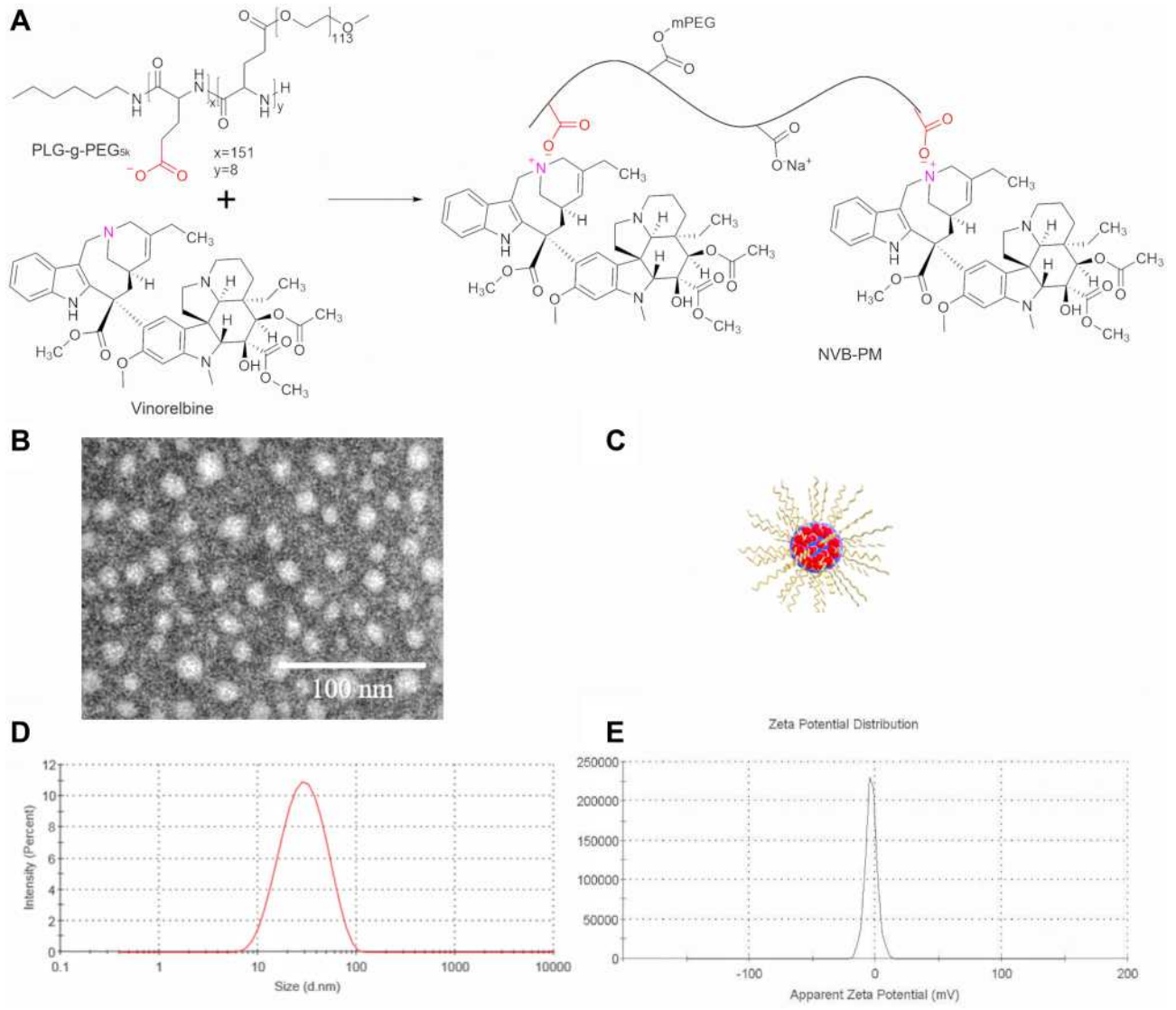

Figure 4 Chemical structures of synthesized and characterization of NVB-PMs. (**A**) Chemical structures of synthesized, (**B**) TEM image, (**C**) schematic illustration, (**D**) size distribution, and (**E**) zeta potential of NVB-PMs. Scale bar, 100 nm.

±5.37% of the NVB were released from CoNP-lips within 48 h. There was no apparent burst release; that is, the release rate from liposomes was much lower than from solution for both drugs, reflecting a sustained release. In plasma, CDDP-PMs and NVB-PMs were stable and were released from their solutions in a sustained fashion; however, different release kinetics were observed in 10% plasma as compared to PBS (Figure 7B). Starting from 8 h, the release rate of CDDP and NVB rapidly increased before reaching a plateau at around 24 h. At 48 h, similar amounts of CDDP and NVB were present in PMs and liposomes,

Table 1 Physicochemical Characteristics of Polymeric Micelle Formulations (n=3)

Polymeric Micelle	Composition	Particle Size, nm	PDI	Zeta Potential, mV	EE, %	DL, %
CDDP-PM	CDDP:PLG-g-PEG$_{5K}$, 1:3 (w/w)	14.57±0.45	0.35±0.023	−4.56±0.22	95.58±1.58	23.57±0.55
NVB-PM	NVB:PLG-g-PEG$_{5K}$, 1:3 (w/w)	24.95±1.14	0.307±0.019	−3.45±0.21	85.62±2.37	19.98±1.11

Note: Data are presented as mean±SD.
Abbreviations: CDDP, cis-diamminedichloroplatinum (II) (cisplatin); DL, drug loading; EE, encapsulation efficiency; NVB, vinorelbine; PDI, polydispersity index; PM, polymeric micelle.

Table 2 Physicochemical Characteristics of Liposome Formulations (n=3)

Liposome	Composition	Particle Size, nm	PDI	Zeta Potential, mV	EE, %		DL, %	
					CDDP	NVB	CDDP	NVB
Blank liposome	E80:cholesterol:DPPG:DSPE-mPEG$_{2000}$, 52:32:14:2 (molar ratio)	149.30±2.46	0.095±0.034	−15.07±0.19	—	—	—	—
CoNP-lip	E80:cholesterol:DPPG:DSPE-mPEG$_{2000}$, 52:32:14:2 (molar ratio)	162.97±9.06	0.17±0.041	−13.02±0.22	59.63±1.53	52.61±2.21	2.14±0.054	3.72±0.15

Note: Data are presented as mean±SD.
Abbreviations: —, no data; CDDP, cis-diamminedichloroplatinum (II) (cisplatin); DL, drug loading; EE, encapsulation efficiency; NVB, vinorelbine; PDI, polydispersity index.

possibly because CoNP-lips were unable to maintain their structure in plasma and ruptured, resulting in the release of PMs. CoNP-lips may thus cause damage to the lipid bilayer, leading to the leakage of active substances. Nonetheless, these results demonstrate that the liposomes can simultaneously release CDDP- and NVB-PMs into the bloodstream for >8 h. To achieve comparable release kinetics, CDDP- and NVB-PMs must be encapsulated in a similar manner. By calculating the cumulative amount of NVB and CDDP released at each time point, we determined that the NVB:CDDP ratio was within the range for synergistic release from CoNP-lips.

The fitting results revealed that the in vitro release profile of CoNp-lips in PBS and 10% plasma followed the Ritger–Peppas equation (Table 3), and according to Ritger–Peppas model theory, the release exponent n was less than 0.43 and drug release mechanism abided by Fick Diffusion.[42]

The sustained release of CDDP and NVB from CoNP-lips could be explained by the strong complexation between CDDP and PLG of the PLG-g-PEG$_{5K}$ in the copolymers, electrostatic force between NVB and PLG-g-PEG$_{5K}$, amount of drug contained in the inner aqueous cavity of the liposome, and effects of negatively charged lipids. NVB and CDDP encapsulated in CoNP-lips are presumably released in 2 steps: first from PMs to the inner core of the liposome, and then into the buffer solution, which could account for their delayed-release kinetics.

Cytotoxicity Analysis

The cytotoxicity of blank liposomes, NP-sol, NP-PMs and CoNP-lips was evaluated in A549 and LLC cells (Figure 8). The blank liposomes had no significant cytotoxic effects after 48 h within the range of tested concentrations. NP-sol, NP-PMs and CoNP-lips showed significant cytotoxicity in A549 cells at the highest concentration (100 μg·mL^{-1}). CoNP-lips and NP-PMs showed similar cytotoxicity to NP-sol, indicating that liposome delivery had no impact on the antitumor effects of CDDP and NVB in A549 cells. In LLC cells, the CoNP-lips and NP-PMs also showed comparable cytotoxicity to NP-sol. However, the IC_{50} of CoNP-lips and NP-PMs was lower than that of NP-sol, possibly because of the sustained release effect and incomplete release of the drugs from liposomes.

Pharmacokinetic Analysis

The pharmacokinetics of CoNP-lips and NP-sol were compared by measuring the CDDP and NVB concentrations in plasma up to 48 h after intravenous administration in rats (Figure 9 and Table 4). The area under the receiver operating characteristic curve ($AUC_{(0-\infty)}$), maximum plasma concentration (C_{max}), half-life ($T_{1/2z}$), and mean retention time (0–∞) of CoNP-lips were much higher than those of NP-sol, while total body clearance (CLz) and apparent volume of distribution (Vz) were lower. The $AUC_{(0-\infty)}$ of NVB and CDDP in CoNP-lips was 6.52- and 8.03-fold higher,

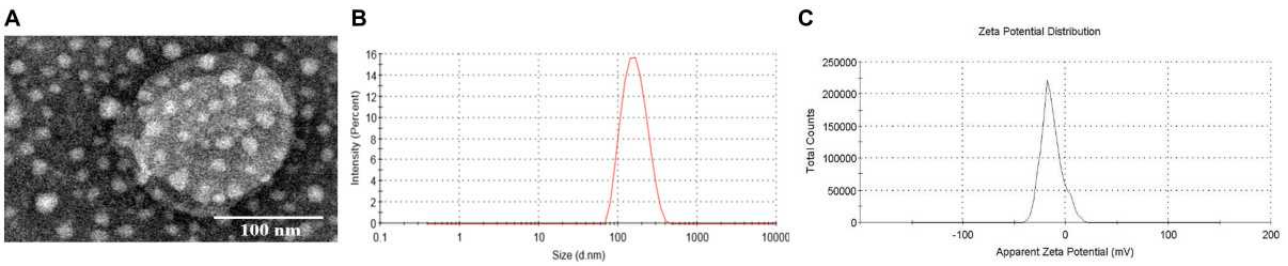

Figure 5 Structural characterization of drug-loaded liposomes. (**A**) TEM images, (**B**) DLS intensity measurements and (**C**) zeta potential of CoNP-lips. Scale bar, 100 nm.

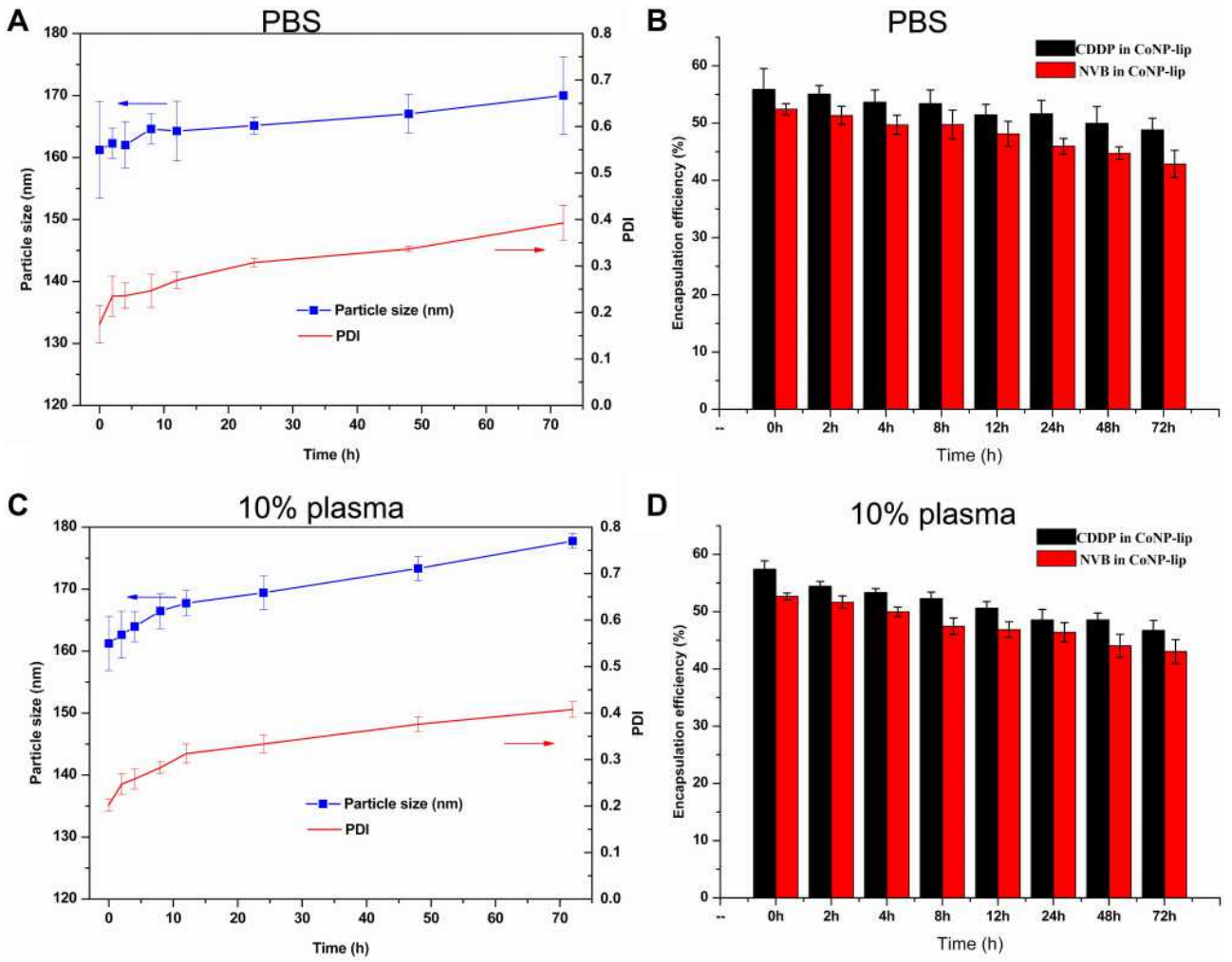

Figure 6 Stability of CoNP-lips in different release media. (**A**) Stability of CoNP-lip particle size and PDI in PBS. (**B**) Efficiency of CDDP and NVB encapsulation in CoNP-lips in PBS at 37°C for up to 72 h. (**C**) Stability of CoNP-lip particle size and PDI in 10% plasma. (**D**) Efficiency of CDDP and NVB encapsulation in 10% plasma in PBS at 37°C for up to 72 h. Data are shown as mean±SD (n=3).

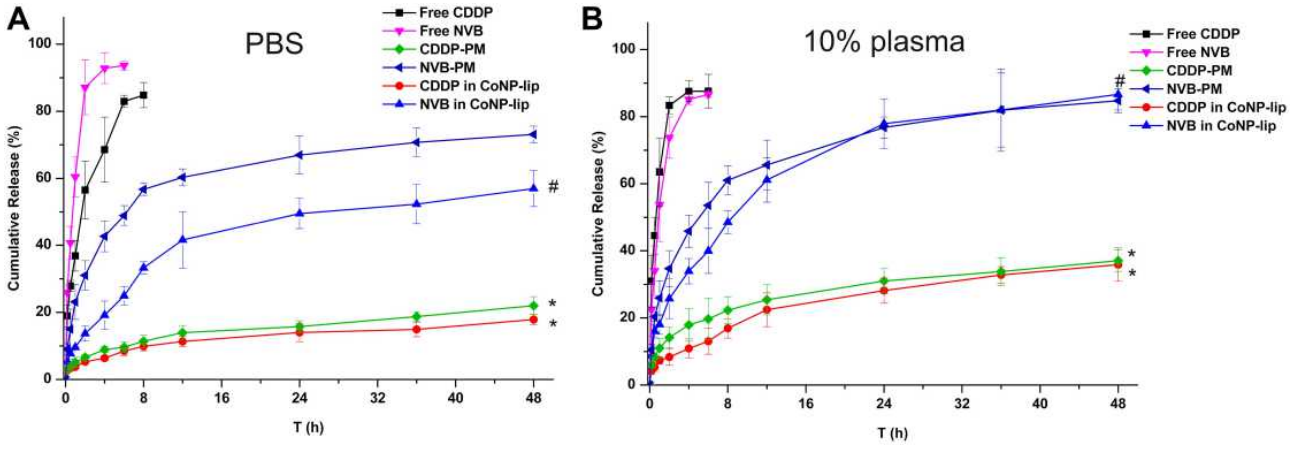

Figure 7 In vitro cumulative release curve. In vitro cumulative release of CDDP and NVB in (**A**) PBS and (**B**) 10% plasma at 37°C. *p<0.05 of indicated groups vs free CDDP, #p<0.05 of indicated groups vs free NVB. Data are shown as mean±SD (n=5).

Table 3 Results of Fitting Models for in vitro Release Profile (n=3)

	Media	Regression Coefficient (R^2)			
		Zero-Order	First-Order	Higuchi	Ritger–Peppas^n
CDDP-PMs	PBS	0.8881	0.8868	0.9843	0.9923, n=0.3651
	10% plasma	0.8333	0.8606	0.9681	0.9966, n=0.3083
NVB-PMs	PBS	0.6579	0.8538	0.8698	0.9296, n=0.2813
	10% plasma	0.7207	0.9249	0.9039	0.9672, n=0.2903
CoNP-lips (CDDP)	PBS	0.8717	0.9071	0.9780	0.9878, n=0.3635
	10% plasma	0.9091	0.9483	0.9874	0.9880, n=0.4271
CoNP-lips (NVB)	PBS	0.8155	0.9288	0.9515	0.9651, n=0.4066
	10% plasma	0.8317	0.9550	0.9640	0.9805, n=0.3794

Abbreviation: n, the diffusional exponent characteristic of the release mechanism in Ritger–Peppas equation.

respectively, whereas C_{max} was 1.08- and 10.43-fold higher, respectively, compared to the values in NP-sol. Additionally, the $T_{1/2z}$ of NVB and CDDP was 6.35- and 2.09-fold longer, respectively, for CoNP-lips than for NP-sol. Thus, the drugs had a longer circulation time when encapsulated into liposomes than when they were freely available in solution. The lower Vz and CLz for CoNP-lips than for NP-sol indicated that encapsulation into liposomes can slow the elimination of NVB and CDDP and thereby prolong their residence time in the blood.

In vivo Antitumor Efficacy

The volume of LLC cell-derived tumors in C57BL/6 mice increased rapidly in the NS group (Figure 10A and C), with an average tumor volume of 1120 mm^3 on day 12 after xenotransplantation. Both CDDP-lips and NVB-lips inhibited tumor growth to some extent. The former had the most potent antitumor effect among the groups compared to NP-sol: the TIR of the CoNP-lip group was 70.29% as compared to 38.45%, 47.78%, and 69.28% in the CDDP-lip, NVB-lip, and NP-sol groups, respectively. As a measure of the in vivo safety of the formulations, body weight showed a declining trend after drug administration, except in the NS group (Figure 10B and D), consistent with the known toxicity of CDDP and NVB. However, the body weight of mice in the CoNP-lip group began to increase after the second injection, eventually reaching the initial value, indicating that the formulation was well tolerated at the tested dose and was less toxic than the drugs in the solution. Moreover, the change in body weight

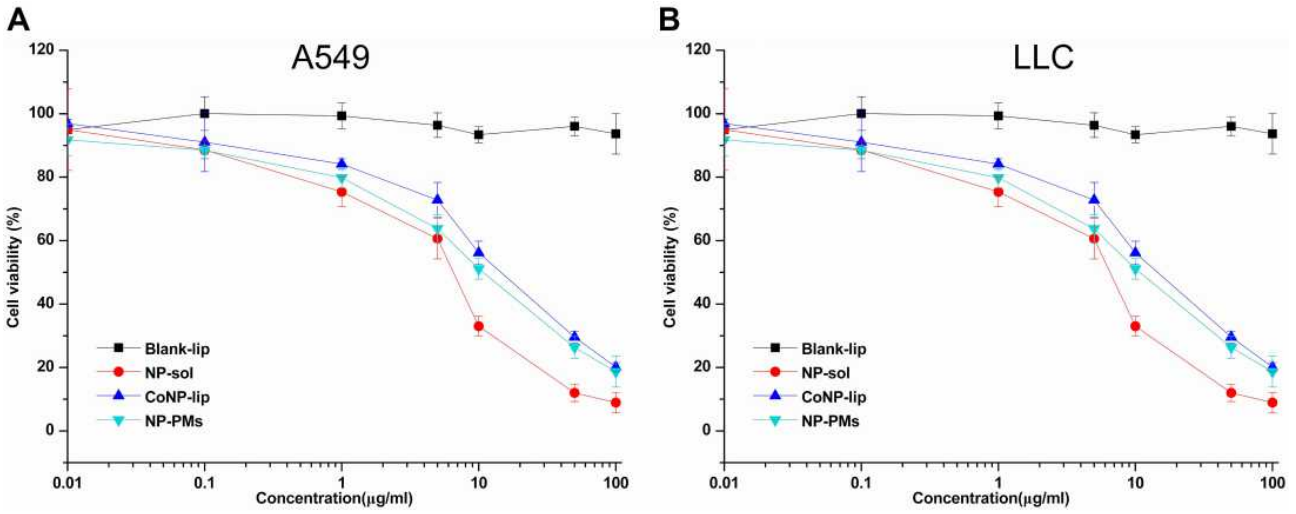

Figure 8 In vitro cytotoxicity of different CoNP-lip formulations in A549 (**A**) and LLC (**B**) cells. The concentration of CDDP is shown on the x-axis; NVB concentration was calculated based on a CDDP/NVB weight ratio of 2:1. Data are shown as mean±SD (n=3).

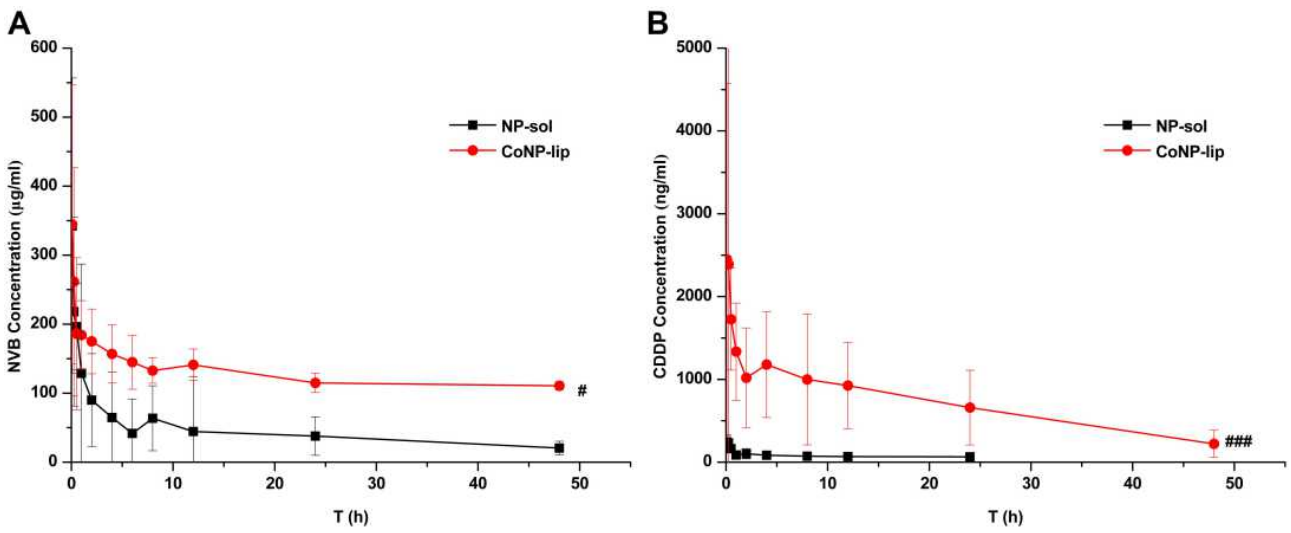

Figure 9 In vivo pharmacokinetic profile of CoNP-lip. Concentration–time profiles of (**A**) NVB and (**B**) CDDP in NP-sol and CoNP-lips following intravenous administration at 5 mg kg^{-1}. *p<0.05 of indicated groups vs free CDDP, #p<0.05, ###p<0.005 of indicated CoNP-lip vs NP-sol. Data are shown as mean±SD (n=5).

of the mice was compatible with the time-to-tumor volume curve after administration.

We evaluated the accumulation of the drugs in tumors and found that the level of CDDP in tumors from NP-sol treated mice decreased after reaching a maximum value at 10 min, while CDDP-lips and CoNP-lip concentrations gradually increased over the same time period (Figure 10E). At 1 h, the tumor levels of CDDP in the CDDP- and CoNP-lip groups were 1.82- and 1.59-fold higher, respectively, than that in the NP-sol group, and at 48 h, the levels were 16.15- and 17.37-fold higher, respectively. Comparable kinetics were observed in the tumor accumulation of NVB: the drug concentration in tumors of the NP-sol group was maximal after 10 min and was higher in the NVB- and CoNP-lip groups than in the NP-sol group, with an increasing trend over time (Figure 10F). These results demonstrate that liposomal encapsulation increases CDDP and NVB accumulation in tumors through passive targeting, thereby enhancing their therapeutic effects.

Conclusion

In this study, we developed NVB and CDDP co-encapsulated liposomes by a reverse evaporation method as a novel type of targeted therapy. Co-delivery of polymeric micelles of vinorelbine and cisplatin, synergistic antitumor efficacy mediated liposomal formulation (E80: cholesterol: DPPG: DSPE-$mPEG_{2000}$, 52: 32: 14: 2) was optimized with BBD. The CI value showed that an NVB: CDDP weight ratio of 2:1 achieved a synergistic antitumor effect in A549 lung adenocarcinoma cells. PLG-g-PEG_{5K} was an ideal nanocarrier for drug delivery in the synthesis of CDDP-PMs and NVB-PMs separately. CoNP-lips had

Table 4 Pharmacokinetic Parameters for NVB and CDDP in NP-Sol and CoNP-Lips Following Intravenous Administration (n=5)

Parameter	NVB		CDDP	
	NP-Sol	CoNP-Lip	NP-Sol	CoNP-Lip
AUC $_{(0-\infty)}$, $\mu g \cdot l^{-1} \cdot h$	4570.90±3415.16	29,899.02±12,716.65**	5080.60±2432.63	40,801.58±25,996.61*
C_{max}, $\mu g \cdot l^{-1}$	362.00±191.17	391.84±173.06	264.59±54.64	2759.84±575.53
$T_{1/2z}$, h	23.14±7.29	146.95±73.82**	19.79±2.50	41.47±4.65
Vz, $l \cdot kg^{-1}$	0.16±0.041	0.069±0.06	48.36±14.03	3.94±2.38**
CLz, $l \cdot h^{-1} \cdot kg^{-1}$	0.18±0.03	0.029±0.054	1.17±0.095	0.17±0.10**
MRT $_{(0-\infty)}$, h	33.11±18.86	212.77±108.74**	25.69±4.83	55.17±13.80

Notes: Data are presented as mean±SD. *P<0.05; **P<0.01 (CoNP-lip vs NP-sol).

Abbreviations: AUC, area under the receiver operating characteristic curve; CDDP, cis-diamminedichloroplatinum (II) (cisplatin); CLz, clearance; C_{max}, maximum plasma concentration; CoNP-lip, vinorelbine and cisplatin co-delivery liposome; MRT, mean residence time; NP-sol, vinorelbine and cisplatin mixed solution; NVB, vinorelbine; $T_{1/2z}$, half-life; Vz, apparent volume of distribution.

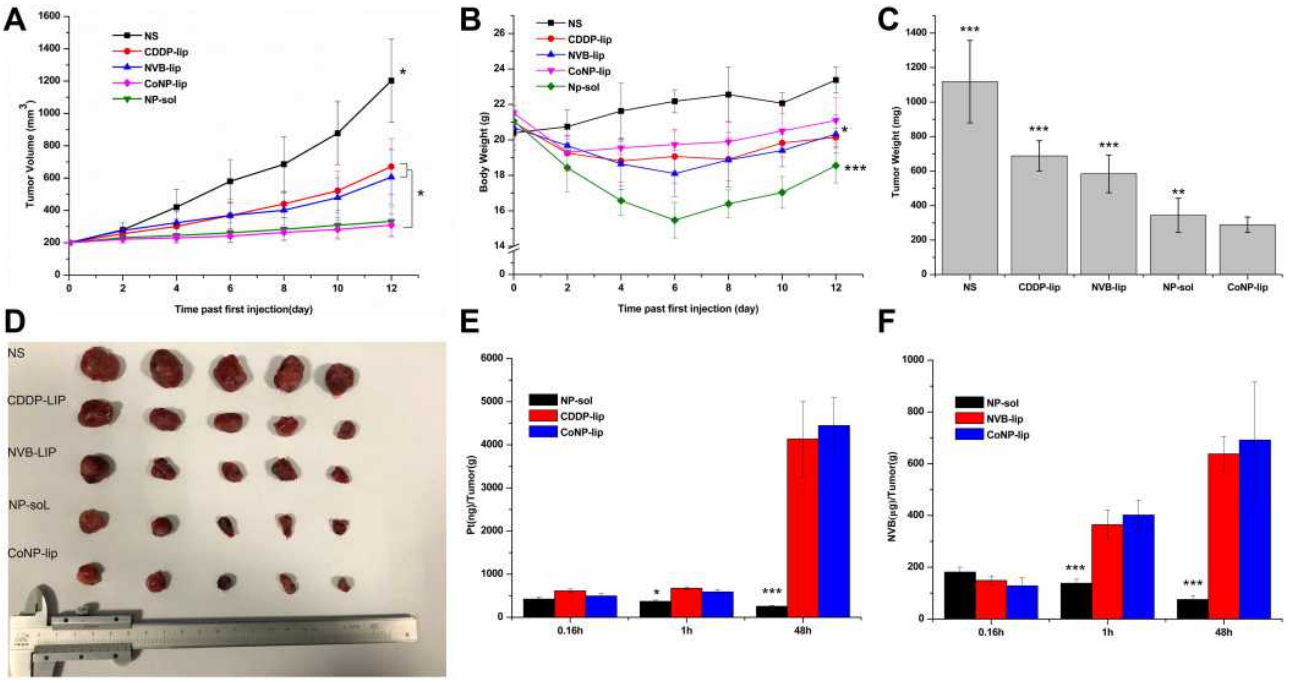

Figure 10 Antitumor efficacy of CoNP-lips in LCC tumor-bearing mice. (**A**) Tumor growth curves of the 5 groups. (**B**) Body weight of tumor-bearing mice during treatment. (**C**) Tumor weight at the end of the experiment. (**D**) Photograph of tumors in the 5 groups. (**E**, **F**) Tumor accumulation of CDDP (**E**) and NVB (**F**). *p<0.05, **p<0.05, ***p<0.005 of indicated groups vs CoNP-lips. Data are shown as mean±SD (n=5).

uniform and appropriate size distribution and exhibited sustained release; moreover, compared to the free drugs in solution, CoNP-lips had greater cytotoxicity in an NSCLC cell line while being less toxic overall (as determined by weight loss) in a mouse xenograft model. These results indicate that the CoNP-lips have clinical potential for the treatment of NSCLC and combination therapy.

Abbreviations

AUC, area under the receiver operating characteristic curve; BBD, Box-Behnken design; CDDP, cis-diammi nedichloroplatinum (II) (cisplatin); CDDP-lip, liposome-encapsulated cisplatin; CI, combination index; CLz, clearance; C_{max}, maximum plasma concentration; CoNP-lip, vinorelbine and cisplatin co-delivery liposome; DL, drug loading; DLS, dynamic light scattering; DMEM, Dulbecco's modified Eagle's medium; DPPG, dipalmitoyl phosphatidylglycerol; DSPE-mPEG$_{2000}$, 1.2-distearoyl-sn-glycero-3-phosphoethanolamine-N-[methoxy(polyethylene glycol)-2000]; E80, egg phosphatidyl lipid-80; EE, entrapment efficiency; EPR, enhanced permeability and retention; FBS, fetal bovine serum; HPLC, high-performance liquid chromatography; IC_{50}, half-maximal inhibitory concentration; LLC, Lewis lung carcinoma; MTT, 3-(4,5-dimethylthiazol-2-yl)-2,5-diphenyltetrazoliumbromide; MWCO, molecular weight cutoff; NP, vinorelbine plus cisplatin; NP-sol, vinorelbine and cisplatin mixed solution; NS, normal saline; NSCLC, non-small cell lung cancer; NVB, vinorelbine; NVB-lip, liposome-encapsulated vinorelbine; PBS, phosphate-buffered saline; PDI, polydispersity index; PEG, polyethylene glycol; PGA, polyglutamic acid; PLG-g-PEG$_{5K}$, sodium poly(α-L-glutamic acid) graft methoxypolyethylene glycol; PM, polymeric micelle; RSM, response surface methodology; TEM, transmission electronic microscopy; TIR, tumor inhibition rate; Vz, apparent volume of distribution.

Acknowledgments

The authors would like to thank the reviewers for their constructive comments to improve the research.

Funding

This work was supported by a grant from National Mega-project for Innovative Drugs of China (no. 2019ZX09721001).

Disclosure

The authors have no conflicts of interest to declare.

References

1. Bray F, Ferlay J, Soerjomataram I, Siegel RL, Torre LA, Jemal A. Global cancer statistics 2018: GLOBOCAN estimates of incidence and mortality worldwide for 36 cancers in 185 countries. *CA Cancer J Clin*. 2018;68:394–424. doi:10.3322/caac.21492
2. Mukherjee A, Paul M, Mukherjee S. Recent progress in the theranostics application of nanomedicine in lung cancer. *Cancers*. 2019;11(5):597. doi:10.3390/cancers11050597
3. Li J, Zhu H, Sun L, Xu W, Wang X. Prognostic value of site-specific metastases in lung cancer: a population based study. *J Cancer*. 2019;10:3079–3086. doi:10.7150/jca.30463
4. Wood DE, Kazerooni EA, Baum SL, et al. Lung cancer screening, version 3.2018. *J Natl Compr Canc Netw*. 2018;16:412–441. doi:10.6004/jnccn.2018.0020
5. Selvi SK, Vinoth A, Varadharajan T, Weng CF, Padma VV. Neferine augments therapeutic efficacy of cisplatin through ROS-mediated non-canonical autophagy in human lung adenocarcinoma (A549 cells). *Food Chem Toxicol*. 2017;103:28–40. doi:10.1016/j.fct.2017.02.020
6. Eldar-Boock A, Polyak D, Scomparin A, Satchi-Fainaro R. Nano-sized polymers and liposomes designed to deliver combination therapy for cancer. *Curr Opin Biotechnol*. 2013;24:682–689. doi:10.1016/j.copbio.2013.04.014
7. Dai W, Wang X, Song G, et al. Combination antitumor therapy with targeted dual-nanomedicines. *Adv Drug Deliv Rev*. 2017;115:23–45.
8. Dasari S, Tchounwou PB. Cisplatin in cancer therapy: molecular mechanisms of action. *Eur J Pharmacol*. 2014;740:364–378. doi:10.1016/j.ejphar.2014.07.025
9. Aapro MS, Harper P, Johnson SA, Vermorken JB. Developments in cytotoxic chemotherapy: advances in treatment utilising vinorelbine. *Crit Rev Oncol Hematol*. 2001;40:251–263. doi:10.1016/S1040-8428(01)00167-6
10. Sugawara S, Maemondo M, Tachihara M, et al. Randomized Phase II trial of uracil/tegafur and cisplatin versus vinorelbine and cisplatin with concurrent thoracic radiotherapy for locally advanced unresectable stage III non-small-cell lung cancer: NJLCG 0601. *Lung Cancer*. 2013;81(1):91–96. doi:10.1016/j.lungcan.2013.04.010
11. Arriagada R, Bergman B, Dunant A, et al. Cisplatin-based adjuvant chemotherapy in patients with completely resected non-small-cell lung cancer. *N Engl J Med*. 2004;350:351–360.
12. Butts CA, Ding K, Seymour L, et al. Randomized phase III trial of vinorelbine plus cisplatin compared with observation in completely resected stage IB and II non–small-cell lung cancer: updated survival analysis of JBR-10. *J Clin Oncol*. 2010;28(1):29–34. doi:10.1200/JCO.2009.24.0333
13. Lilenbaum RC, Herbst RS. Vinorelbine and gemcitabine combinations in advanced non small-cell lung cancer. *Clin Lung Cancer*. 2001;2:123–127. doi:10.3816/CLC.2000.n.024
14. Ud DF, Waqar A, Izhar U, et al. Effective use of nanocarriers as drug delivery systems for the treatment of selected tumors. *Int J Nanomedicine*. 2017;12:7291–7309. doi:10.2147/IJN.S146315
15. Yu H, Tang Z, Li M, et al. Cisplatin loaded poly(L-glutamic acid)-g-methoxy poly(ethylene glycol) complex nanoparticles for potential cancer therapy: preparation, in vitro and in vivo evaluation. *J Biomed Nanotechnol*. 2016;12:69–78. doi:10.1166/jbn.2016.2152
16. Chenguang Y, Wantong S, Dawei Z, et al. Poly (l-glutamic acid)-g-methoxy poly (ethylene glycol)-gemcitabine conjugate improves the anticancer efficacy of gemcitabine. *Int J Pharm*. 2018;550:79–88. doi:10.1016/j.ijpharm.2018.08.037
17. Reithofer MR, Chan K-H, Lakshmanan A, et al. Ligation of anti-cancer drugs to self-assembling ultrashort peptides by click chemistry for localized therapy. *Chem Sci*. 2014;5:625–630. doi:10.1039/C3SC51930A
18. Chan KH, Lee WH, Ni M, et al. C-terminal residue of ultrashort peptides impacts on molecular self-assembly, hydrogelation, and interaction with small-molecule drugs. *Sci Rep*. 2018;8:17127. doi:10.1038/s41598-018-35431-2
19. Maruyama K. Intracellular targeting delivery of liposomal drugs to solid tumors based on EPR effects. *Adv Drug Deliv Rev*. 2011;63(3):161–169. doi:10.1016/j.addr.2010.09.003
20. Crommelin DJA, van Hoogevest P, Storm G. The role of liposomes in clinical nanomedicine development. What now? Now what? *J Control Release*. 2020;318:256–263. doi:10.1016/j.jconrel.2019.12.023
21. Maeda H, Bharate GY, Daruwalla J. Polymeric drugs for efficient tumor-targeted drug delivery based on EPR-effect. *Eur J Pharm Biopharm*. 2009;71(3):409–419. doi:10.1016/j.ejpb.2008.11.010
22. Bozzuto G, Molinari A. Liposomes as nanomedical devices. *Int J Nanomedicine*. 2015;10:975–999. doi:10.2147/IJN.S68861
23. Maakaron JE, Mims AS. Daunorubicin-cytarabine liposome (CPX-351) in the management of newly diagnosed secondary AML: a new twist on an old cocktail. *Best Pract Res Clin Haematol*. 2019;32(2):127–133. doi:10.1016/j.beha.2019.05.005
24. Camacho KM, Menegatti S, Vogus DR, et al. DAFODIL: a novel liposome-encapsulated synergistic combination of doxorubicin and 5FU for low dose chemotherapy. *J Control Release*. 2016;229:154–162. doi:10.1016/j.jconrel.2016.03.027
25. Karpuz M, Silindir-Gunay M, Kursunel MA, Esendaglic G, Dogand A, Ozer AY. Design and in vitro evaluation of folate-targeted, co-drug encapsulated theranostic liposomes for non-small cell lung cancer. *J Drug Deliv Sci Technol*. 2020;57:101707. doi:10.1016/j.jddst.2020.101707
26. Karpuz M, Silindir-Gunay M, Ozer AY, et al. Diagnostic and therapeutic evaluation of folate-targeted paclitaxel and vinorelbine encapsulating theranostic liposomes for non-small cell lung cancer. *Eur J Pharm Sci*. 2020;156:105576. doi:10.1016/j.ejps.2020.105576
27. Chou TC. Drug combination studies and their synergy quantification using the chou-talalay method. *Cancer Res*. 2010;70:440–446. doi:10.1158/0008-5472.CAN-09-1947
28. Chen Q, Luo L, Xue Y, et al. Cisplatin-loaded polymeric complex micelles with a modulated drug/copolymer ratio for improved in vivo performance. *Acta Biomater*. 2019;92:205–218. doi:10.1016/j.actbio.2019.05.007
29. Wang J, Xing XQ, Fang XC, et al. Cationic amphiphilic drugs self-assemble to the core-shell interface of PEGylated phospholipid micelles and stabilize micellar structure. *Philos Trans a Math Phys Eng Sci*. 2013;371:20120309. doi:10.1098/rsta.2012.0309
30. Wang Y, Wang R, Lu X, et al. Pegylated phospholipids-based self-assembly with water-soluble drugs. *Pharm Res*. 2010;27(2):361–370. doi:10.1007/s11095-009-0029-6
31. Bonde S, Bonde CG, Prabhakar B. Quality by design based development and validation of HPLC method for simultaneous estimation of paclitaxel and vinorelbine tartrate in dual drug loaded liposomes[J]. *Microchem J*. 2019;149:103982. doi:10.1016/j.microc.2019.103982
32. Hang X, Lu Z, Lin L, et al. Membrane-loaded doxorubicin liposomes based on ion-pairing technology with high drug loading and pH-responsive property. *AAPS PharmSciTech*. 2016;18:2120–2130. doi:10.1208/s12249-016-0693-x
33. Zalba S, Navarro I, Troconiz IF, Tros de Ilarduya C, Garrido MJ. Application of different methods to formulate PEG-liposomes of oxaliplatin: evaluation in vitro and in vivo. *Eur J Pharm Biopharm*. 2012;81:273–280. doi:10.1016/j.ejpb.2012.02.007
34. Liu X, Han M, Xu J, et al. Asialoglycoprotein receptor-targeted liposomes loaded with a norcantharimide derivative for hepatocyte-selective targeting. *Int J Pharm*. 2017;520(1–2):98–110. doi:10.1016/j.ijpharm.2017.02.010
35. Su M, Zhao M, Luo Y, et al. Pharmacokinetics and tissue distribution of vinorelbine delivered in parenteral lipid emulsion. *Eur J Lipid Sci Technol*. 2011;113(2):152–159. doi:10.1002/ejlt.201000433

36. Lu XY, Zhang FY, Qin L, Xiao FY, Liang W. Polymeric micelles as a drug delivery system enhance cytotoxicity of vinorelbine through more intercellular accumulation. *Drug Deliv.* 2010;17(4):255–262. doi:10.3109/10717541003702769
37. Ghosh S. Cisplatin: the first metal based anticancer drug. *Bioorg Chem*. 2019;88:102925.
38. Sorensen SF, Carus A, Meldgaard P. Intravenous or oral administration of vinorelbine in adjuvant chemotherapy with cisplatin and vinorelbine for resected NSCLC. *Lung Cancer.* 2015;88 (2):167–173. doi:10.1016/j.lungcan.2015.02.010
39. Lee CT, Huang YW, Yang CH, Huang KS. Drug delivery systems and combination therapy by using vinca alkaloids. *Curr Top Med Chem*. 2015;15:1491–1500. doi:10.2174/1568026615666150414120547
40. Marzban E, Alavizadeh SH, Ghiadi M, et al. Optimizing the therapeutic efficacy of cisplatin PEGylated liposomes via incorporation of different DPPG ratios: in vitro and in vivo studies. *Colloids Surf B Biointerfaces*. 2015;136:885–891. doi:10.1016/j.colsurfb.2015.10.046
41. Zahednezhad F, Zakeri-Milani P, Mojarrad JS, Valizadeh H. The latest advances of cisplatin liposomal formulations: essentials for preparation and analysis. *Expert Opin Drug Deliv.* 2020;17 (4):523–541. doi:10.1080/17425247.2020.1737672
42. Ritger Philip L, Peppas NA. A simple equation for description of solute release II. Fickian and anomalous release from swellable devices. *J Control Release*. 1987;5:37–42. doi:10.1016/0168-3659(87)90035-6